bottom at station 185 (15 km northeast of station 186) averaged 23 cm sec^{-1} toward 300° during the time measurements were being taken at station 186 and averaged 2.3 cm sec^{-1} toward the east at station 187. These observations lasted for only half a semidiurnal tidal cycle and do not represent the average current regime in the region. The main deep current in this region is the Western Boundary Undercurrent (WBUC). The southwesterly trending WBUC might well transport such patches of turbid water along the continental margin after the turbidity flow has expended most of its forward momentum near the edge of the abyssal plain.

Seismograph records at Lamont-Doherty Geological Observatory have been examined for the period 25 April to 8 May 1971 (2 weeks prior to the date of the measurements made at station 186) for evidence of significant seismic activity in the Grand Banks area. No such activity was detected (*14*).

We believe that other isolated patches of highly turbid bottom water that have been found along the western margin of the North American basin should also be considered in this light (*4–8*). It may not be necessary to have very high bottom currents actively eroding the substrate at the site of observation to account for the high concentrations of particulate matter in some bottom waters.

ANTHONY F. AMOS
Port Aransas Marine Laboratory,
University of Texas Marine Science
Institute, Port Aransas 78373
ROBERT D. GERARD
Lamont-Doherty Geological
Observatory, Columbia University,
Palisades, New York 10964

References and Notes

1. B. C. Heezen and M. Ewing, *Am. J. Sci.* **250**, 849 (1952).
2. B. C. Heezen and C. D. Hollister, *The Face of the Deep* (Oxford Univ. Press, New York, 1971), pp. 283–333.
3. P. E. Biscaye and S. L. Eittreim, *Mar. Geol.* **23**, 155 (1977).
4. D. A. Johnson and P. F. Lonsdale, *Deep-Sea Res.* **23**, 429 (1976).
5. W. S. Broecker, T. Takahashi, Y.-H. Li, *ibid.*, p. 1083.
6. W. S. Broecker and A. Bainbridge, *J. Geophys. Res.* **83**, 1963 (1978).
7. L. Armi, *ibid.*, p. 1971.
8. P. E. Biscaye and S. L. Eittreim, in *Suspended Solids in Water*, R. Gibbs, Ed. (Plenum, New York, 1974), p. 227.
9. P. G. Brewer, D. W. Spencer, P. E. Biscaye, A. Hanley, P. L. Sachs, C. L. Smith, S. Kadar, J. Fredericks, *Earth Planet. Sci. Lett.* **32**, 393 (1976).
10. P. E. Biscaye and C. R. Olsen, *Am. Soc. Limnol. Oceanogr. Spec. Symp.* **2**, 124 (1976).
11. A. F. Amos, *The New York Bight and Hudson Canyon in October 1974* (Technical Report COO-2185-10, Lamont-Doherty Geological Observatory, Palisades, N.Y., 1976), pp. 150–180.
12. An acoustic "pinger" was used to prevent our instrument package from touching bottom and stirring up sediment. Two of the highly turbid samples (station 186) were collected in bottles attached to the wire above our STD instrument, one sample (station 186) was collected in a "rosette" sampler bottle surrounding the STD, and one sample (station 185) was collected 15 km away. Thus, contamination of stirred-up sediment is improbable. The closest approach to the bottom at station 186 was 4 m.
13. A. F. Amos, A. L. Gordon, E. D. Schneider, *Deep-Sea Res.* **18**, 145 (1971); L. Armi and R. C. Millard, *J. Geophys. Res.* **81**, 4983 (1976).
14. L. Sykes, personal communication.
15. B. C. Heezen and M. Tharp, *Physiographic Diagram of the North Atlantic Ocean* (Geological Society of America map, Boulder, Colo., 1968).
16. Anonymous, *Proceedings of the National Oceanographic Instrumentation Center Turbidity Workshop*, Washington, D.C., 6–8 May 1974.
17. We thank E. Escowitz and the Global Ocean Floor Analysis and Research group at the Naval Oceanographic Office, Chesapeake Beach, Md. (1971), facility who made available to us the U.S.N.S. *Lynch*. This work was supported by Energy Research and Development Administration contract AT(11-1) 2185. University of Texas Marine Science Institute contribution 306. Lamont-Doherty Geological Observatory contribution 2747.

7 July 1978; revised 11 September 1978

Generation of Oil-Like Pyrolyzates from Organic-Rich Shales

Abstract. *Pyrolyzates similar to natural crude oils were generated from organic-rich shales by hydrous pyrolysis. With this type of pyrolysis it is possible to make more sophisticated correlations between crude oils and their source rocks, evaluate the hydrocarbon potential of a source rock, and elucidate the variables involved in the natural oil-generating process.*

The products generated by anhydrous pyrolysis and retorting of organic-rich shales contain significant amounts of olefins (Fig. 1). The rarity of olefins in natural crude oils (*1*) indicates that these pyrolysis methods do not duplicate the natural oil-generating process. In June 1977 we generated pyrolyzates that did not contain olefins from organic-rich shales (Fig. 1). In addition, the pyrolyzates had other properties that closely match those of natural crude oils. The process, called hydrous pyrolysis, involves filling half of a pressure vessel with equal volumes of water and crushed or sawed blocks of organic-rich shale. The remaining void is filled with helium at 1 to 2 atm, and the vessel is then heated to 330°C for 3 to 4 days.

The organic-rich shales used in this process are in their prehydrocarbon generation stage of diagenesis. This is evaluated before pyrolysis by elemental analyses and visual analysis of the kerogen portion of the organic matter (*2–5*). Oil-like pyrolyzates have been generated by this process from shales containing algal and liptinitic kerogens. Woodford Shale from Carter County, Oklahoma, which contains liptinitic kerogen and 4.3 percent (by weight) organic carbon, is used in this report as an example of hydrous pyrolysis.

A gas chromatogram of the pyrolyzate generated by hydrous pyrolysis of Woodford Shale (Fig. 2A) is similar to that of a natural crude oil (Fig. 2B) that has been geochemically correlated (*6*)

Table 1. Comparison of natural crude oils with pyrolyzates generated by hydrous pyrolysis.

Substance	*n*-Alkane range	CPI*	Pristane/phytane ratio	Optical rotation	$\delta^{13}C$ (PDB)†
Natural Woodford crude oils	C_1 to C_{37}	1.0	1.4 to 1.5	0.1 to 0.3	−29.8 to −30.0
Pyrolyzates from hydrous pyrolysis of Woodford Shale	C_1 to C_{37}	1.0 to 1.1	1.1 to 2.3	0.1 to 0.2	−29.4 to −30.0
Crude oils (overall range)	C_1 to C_{37}	0.8 to 1.2	0.4 to 8.0	−0.1 to 4.5	−21.0 to −35.0

*Carbon preference index (CPI) = $\frac{1}{2}[(C_{25} + C_{27} + C_{29})/(C_{24} + C_{26} + C_{28}) + (C_{25} + C_{27} + C_{29})/(C_{26} + C_{28} + C_{30})]$. †Per mil increment in ^{13}C relative to Pee Dee belemnite.

Table 2. Composition of natural crude oils and pyrolyzates generated by hydrous pyrolysis at 330°C for 96 hours. Values are percentages by weight.

Substance	Eluted fraction* (%)				Non-eluted† fraction (%)
	Saturates	Aromatics	Polars	Total	
Natural Woodford crude oils	80–89	10–16	1–4	100	0
Pyrolyzates from hydrous pyrolysis of Woodford Shale	62	28	10	62	38

*Portion eluted on an activated alumina column with *n*-heptane (saturates), dichloromethane (aromatics), and dichloromethane-methanol mixtures (polars). †Portion not eluted on an activated alumina column with dichloromethane-methanol mixtures.

Fig. 1. Ternary diagram showing the compositions of pyrolyzates generated by different pyrolysis and retorting methods with natural crude oils. (○) Class I retorting of Green River Shale (*10, 17*); (◑) class II retorting of Green River Shale (*17*); (◒) class III retorting of Green River Shale (*17*); (●) hydrogasification of Green River Shale (*9*); (□) anhydrous vacuum pyrolysis of Green River Shale (*12*); (■) Fischer assay of Green River Shale (*17*); (△) hydrous pyrolysis of Woodford Shale; and (▽) hydrous pyrolysis of Green River Shale.

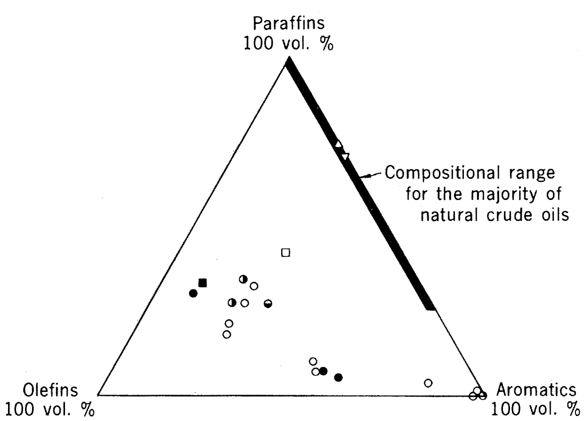

with the Woodford Shale. Conversely, the gas chromatogram of the product generated by pyrolysis without water (Fig. 2C) is distinctly different. Additional similarities between pyrolyzates and crude oils from Woodford sources are shown in Table 1. The wide range in the pristane/phytane ratio of the pyrolyzate appears to be dependent on the duration of the experiment. Although the temperature used for hydrous pyrolysis may be 200° to 250°C higher than that inferred for natural petroleum generation (*7, 8*), the similarities between the pyrolyzate and natural crude oils suggest that hydrous pyrolysis approaches duplication of the natural process. The higher temperature used during hydrous pyrolysis increases the reaction rate, but differences between the gross properties of the pyrolyzate and the natural product are apparently minor.

Table 3. Total yields of expelled pyrolyzate phases from Woodford Shale at 330°C for 72 hours. Values are percentages (by weight) of whole rock.

Expelled pyrolyzate phases*	Hydrous pyrolysis	Anhydrous + helium-pressured pyrolysis†	Anhydrous pyrolysis
Free	1.5	0.0	0.0
Sorbed	0.6	0.5	0.1
Aqueous	0.01	0.0	0.0
Gas	0.7	0.7	2.1
Total	2.8	1.2	2.2

*Free phase, pyrolyzate layer on top of water; sorbed phase, pyrolyzate film on shale chips; aqueous phase, pyrolyzate dissolved in water; and gas phase, pyrolyzate in the gaseous phase. †Helium pressure at 330°C is 140 atm.

Table 4. Hydrogen budget of hydrous and anhydrous pyrolysis. Values are moles per 100 g of Woodford Shale measured at 25°C, except where noted otherwise.

Hydrogen form	Amount (moles per 100 g × 10³)		
	Hydrous	Anhydrous	ΔH_2 (hydrous − anhydrous)
H_2 (gas)	5.67	4.82	0.85
H_2S (gas)	0.84	9.80	−8.96
$2H^+$ (aq)*	0.08×10^{-3}	0.00	0.08×10^{-3}
H_2S (aq)†	0.08	0.00	0.08
Total H_2	6.59	14.62	−8.03

*Abbreviation: aq, aqueous. †Calculated from thermodynamic data.

Two noticeable differences are the larger noneluted fraction of the pyrolyzate and its slightly lower content of saturated compounds in the eluted fraction (Table 2). The pyrolyzates are under considerably lower pressure than natural crude oils and migrate relatively short distances. The noneluted fraction is quite polar, and in the natural system it may not be expelled from the shale or it may be chromatographically removed during migration. The higher temperatures used in hydrous pyrolysis are another possible cause of this deviation. The smaller portion of saturates in the eluted fraction of the pyrolyzate is probably a result of the higher temperature used. Studies of retorting of shales have shown that the content of saturates decreases with increasing retorting temperatures (*9, 10*).

Hydrous pyrolysis differs from other pyrolysis methods in the following way: during hydrous pyrolysis shale and its organic constituents are in contact with liquid water (*11*) at a pressure of more than 127 atm; in other pyrolysis methods shale is surrounded by a vacuum (*12*), nitrogen (*13*), or inert gas (*14*) at essentially 1 atm. Whether liquid water is important as a reactant or because of its confining and pressuring effect, or both, is not yet known. The presence of bulk liquid water apparently results in the best product in greatest yield (Table 3). On the other hand, some oil-like pyrolyzate was generated at 330°C from Woodford Shale, using helium to provide a reactor pressure similar to the water vapor pressure. It is not yet clear whether the helium pressure inhibits escape of pyrolysis products into the bulk vapor space, keeping them where they can react with other pyrolysis products in the rock, or alters factors other than the behavior of the organic phase, giving products different from those produced at low pressure. Harwood (*15*) showed that in anhydrous vacuum pyrolysis of kerogen more than 50 percent (by volume) of the evolved gas may be hydrogen. Confinement of hydrogen within the rock by external pressure could be critical to the hydrogenation of olefins in the pyrolyzate. The hydrogen budget in Table 4 shows that sufficient hydrogen is generated during both hydrous and anhydrous pyrolysis.

A practical advantage of hydrous pyrolysis is that representative liquid product forms a layer on top of the water in the pressure vessel and may be easily removed with a pipette for analysis (*16*). The pyrolyzate from helium-pressured pyrolysis occurs as a liquid film on the shale chips, which must be removed by quickly rinsing the chips with an organic solvent such as benzene or methylene chloride. This type of pyrolysis is less precise, is subject to loss of lower-boiling products, and does not give a good indication of the amount of pyrolyzate that may be expelled from a particular type of shale.

The pyrolyzate apparently migrates out of the shale as a separate phase, not

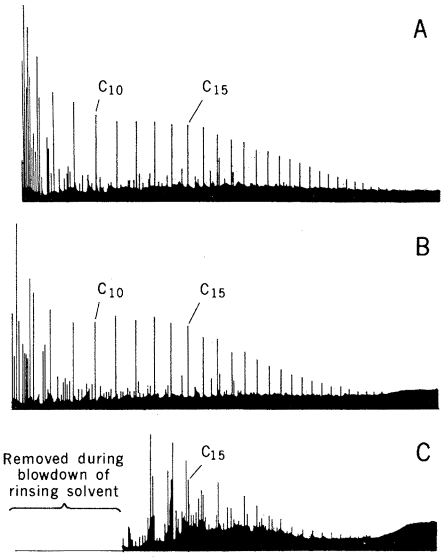

Fig. 2. Gas chromatograms of (A) pyrolyzate generated from Woodford Shale by hydrous pyrolysis at 330°C for 72 hours, (B) natural Woodford crude oil, and (C) pyrolyzate generated from Woodford Shale by anhydrous pyrolysis at 330°C for 72 hours.

miscible with water. Petrographic examination of thin sections of hydrous pyrolyzed shale shows that the liquid product fills wavy fractures that are parallel to and sharp-sided fractures that are perpendicular to the linear fabric of the shale. In some fractures the filling may be traced to the edge of a shale block, where the pyrolyzate continues as a thin film. We observed some of these textural features in shales from cores and outcrops.

Hydrous pyrolysis may prove to be a sophisticated method for correlating crude oils with their source rocks and evaluating the generating capability of a source rock. It should provide more information on the natural oil-generating processes and the dependence of the composition of crude oil on such variables as temperature, pressure, time, and water. It may also help to elucidate the primary migration mechanisms of crude oils in their source rocks.

M. D. LEWAN
J. C. WINTERS, J. H. MCDONALD
Amoco Production Company Research Center, Tulsa, Oklahoma 74102

References and Notes

1. T. Hoering, *Chem. Geol.* **20**, 1 (1977).
2. B. Tissot, B. Durand, J. Espitalie, A. Combaz, *Bull. Am. Assoc. Pet. Geol.* **58**, 499 (1974).
3. W. G. Dow, *J. Geochem. Explor.* **7**, 79 (1977).
4. K. E. Peters, R. Ishiwatari, I. R. Kaplan, *Bull. Am. Assoc. Pet. Geol.* **61**, 504 (1977).
5. F. L. Staplin, *Bull. Can. Pet. Geol.* **17**, 4766 (1969).
6. For current geochemical correlation techniques see J. Williams, *Bull. Am. Assoc. Pet. Geol.* **58**, 1243 (1974).
7. G. Philippi, *Geochim. Cosmochim. Acta* **19**, 1021 (1965).
8. J. Connan, *Bull. Am. Assoc. Pet. Geol.* **58**, 2516 (1974).
9. F. Schora, Jr., H. Feldkirchner, P. Tarman, S. Weil, *Hydrocarbon Process.* **54**, 89 (April 1974).
10. R. Gustafson, in *Encyclopedia of Chemical Technology*, R. E. Kirk and D. F. Othemer, Eds. (Interscience, New York, 1969), vol. 18, p. 120.
11. At 25°C and 1 atm the total volume of shale and liquid water is about half that of the pressure vessel. During pyrolysis (330°C) the shale is completely submerged in the expanded liquid water phase, and the remaining void space has a vapor pressure of at least 127 atm. This pressure is the result of water vapor. Higher pressures may occur, depending on the amount of gases and liquids that evolve from the shale.
12. A. Douglas, G. Eglinton, W. Henderson, in *Advances in Organic Geochemistry*, G. Hobson and G. Speers, Eds. (Pergamon, Oxford, 1966), pp. 369–388.
13. R. Ishiwatari, M. Ishiwatari, B. Rohrback, I. Kaplan, *Geochim. Cosmochim. Acta* **41**, 815 (1977).
14. S. Martin, in *Advances in Organic Geochemistry*, R. Campos and J. Goni, Eds. (Empresa Nacional Adaro De Investigaciones Mineras, 1975), pp. 677–692.
15. R. J. Harwood, *Bull. Am. Assoc. Pet. Geol.* **61**, 2082 (1977).
16. Sufficient yields of analytical work usually require a 500-ml or 1-liter pressure vessel, depending on the organic richness of the rock.
17. G. Dinneen, R. Van Meter, J. Smith, C. Bailey, G. Cook, C. Albright, J. Ball, *U.S. Bur. Mines Bull. 593* (1961), p. 14.
18. We thank the Amoco Production Company Research and Development Department management for support of this basic research and permission to publish results at an early stage of the work.

5 June 1978; revised 27 November 1978

Atmospheric Halocarbons, Hydrocarbons, and Sulfur Hexafluoride: Global Distributions, Sources, and Sinks

Abstract. *The global distribution of fluorocarbon-12 and fluorocarbon-11 is used to establish a relatively fast interhemispheric exchange rate of 1 to 1.2 years. Atmospheric residence times of 65 to 70 years for fluorocarbon-12 and 40 to 45 years for fluorocarbon-11 best fit the observational data. These residence times rule out the possibility of any significant missing sinks that may prevent these fluorocarbons from entering the stratosphere. Atmospheric measurements of methyl chloroform support an 8- to 10-year residence time and suggest global average hydroxyl radical (HO) concentrations of* 3×10^5 *to* 4×10^5 *molecules per cubic centimeter. These are a factor of 5 lower than predicted by models. Additionally, methyl chloroform global distribution supports Southern Hemispheric HO levels that are a factor of 1.5 or more larger than the Northern Hemispheric values. The long residence time and the rapid growth of methyl chloroform cause it to be a potentially significant depleter of stratospheric ozone. The oceanic sink for atmospheric carbon tetrachloride is about half as important as the stratospheric sink. A major source of methyl chloride* (3×10^{12} *grams per year), sufficient to account for nearly all the atmospheric methyl chloride, has been identified in the ocean.*

A major uncertainty in the fluorocarbon-ozone theory has been due to insufficient and often conflicting data on the global distribution of halocarbons. Calculation of the residence time of fluorocarbons is critically linked with this distribution and is an essential input into models that attempt to simulate the stratospheric O_3 depletion problem (*1*, *2*). In addition, the budgets and distributions of halocarbons provide a unique means for studying some of the fundamental features of the natural atmosphere. Inert species such as fluorocarbons and SF_6 are tracers that identify and quantify the global circulation, whereas the distribution of the more reactive halocarbons such as methyl chloroform (CH_3CCl_3) offers a unique means for quantifying the role of the hydroxyl radical (HO), a central atmospheric species that cleanses the atmosphere of impurities (*3*, *4*). Because a comprehensive set of global data on the distribution of unreactive and reactive halocarbons has not been available, most estimates have been made from point measurements and the hemispheres have been assumed to be well mixed. We present here extensive global measurements, which substantially alleviate this deficiency and provide an essential means for developing and verifying two-dimensional global photochemical models that are in a state of active development. We also characterize the growth of important atmospheric halocarbons, including several fluorocarbons, on the basis of data collected over a period of 3 years, and we discuss the important role the oceans play in the atmospheric chlorine budget.

We determined the global distributions of a large number of trace constituents between 64°N and 90°S at widely varying longitudes (*5*). We analyzed these background air samples both in situ and by collecting pressurized air samples in specially constructed stainless steel and glass vessels. All the in situ air and seawater analyses were conducted aboard a U.S. Coast Guard vessel, the *Burton Island*, which sailed the Pacific from Oakland, California (37°N), to Wellington, New Zealand (42°S). We took surface seawater samples in the Pacific Ocean from depths of 0 to 300 m at 50-m intervals. We also conducted several short-term field studies in clean remote sites on the west coast of the United States, starting in November 1975. Electron capture and flame ionization gas chromatographic techniques were used to analyze halogenated species and hydrocarbons, respectively. Details of the measurement methods are given in (*6*, *7*).

Figure 1 shows the global distribution of five fluorinated species (F stands for fluorocarbon): F12 (CCl_2F_2), F11 (CCl_3F), F113 (CCl_2FCClF_2), F114 ($CClF_2CClF_2$), and SF_6. All these species are man-made, are emitted predominately in the Northern Hemisphere (NH), and are essentially inert in the troposphere. It is clear from Fig. 1 that all five species are well mixed within each hemisphere and that the average concentrations in the Southern Hemisphere (SH) differ only marginally (10 to 15 percent) from the NH values.

Using a simple two-box model (*4*) and the emissions data for F12 and F11 (*8*), we calculate an interhemispheric exchange rate (τ_e) of 1 to 1.2 years. This is in good agreement with estimates by Czeplak and Junge (*9*) but in disagreement with other studies that calculate τ_e values of 2 to 4 years (*9*). Thus, the fluorocarbon data suggest that NH and SH air masses are exchanged in a rela-

0036-8075/79/0302-0899$00.50/0